Relationship between some selected major, minor and trace elements in the IOCG deposits (on the example of the unique Sin Quyen deposit, Lao Cai province, north Vietnam)

H. Duong Van[1], C. Nguyen Dinh [2*], A. Piestrzynski[2], J. Pieczonka[2]

[1] *University of Mining and Geology (UMG), Hanoi, Vietnam*

[2]*AGH University of Science and Technology (AGH-UST), Krakow, Poland*

cnd@agh.edu.pl

Abstract

In the paper the authors attempted to study the relations between several selected elements present in the IOCG Sin Quyen deposit, Lao Cai, North Vietnam and to interpret the obtained correlations especially with coefficient higher than 0.7. The correlations with high coefficients are mainly observed for the elements belonging to the chalcophile group (Cu, Ag, Au, Te, Bi) and for the relation between uranium and Ag, Au, Cu, Pb and Bi .But the S and Fe as well as REE currying minerals are predominant in the studied deposit, but no strong correlation between them and other elements was observed even with Cu. The phenomena primarily explained based on the geochemistry properties of the mentioned elements and the characteristics of IOCG deposits.

Keywords: IOCG Sin Quyen deposit, correlations, geochemistry

Introduction

Generally the IOCG deposits are known as the deposits with the elevated contents of Cu, Au, Ag, REE, U, P and Co. They are controlled structurally or stratigraphically and temporally and spatially associated with presence Na-Ca-K alteration (Barton, 2014). According to numerous scientists the IOCG deposits could be formed as a consequence of processes as: (1) magmatic hydrothermal fluid activity, (2) metamorphic hydrothermal fluids derived from crustal source at depth, and (3) terrestrial hydrothermal fluids circulated by intrusive or crustal heat (Hitzman et al., 1992; Groves et al., 2010). The mineral and chemical composition spectra of the IOCG deposits are very inhomogeneous even within one area (Li et al., 2014). The variety both in mineral composition and in ore distribution within a deposit can be connected with many periods of the magmatism activity and geological forming structures. The inhomogeneous are also reflected in variable ratios of different elements: Cu/Au, Au/Ag and so on (Ivan et al., 2002; Zhu, 2016). Depending on the local geological conditions, the IOCG deposits can be poor or rich in Fe, Cu or other mentioned elements (Requia and Fontbote, 2000; Gandhi, 2003; Requia et al., 2003). Therefore not only Fe or Cu can be a main mined ores, but also Au, Ag, U or REE are as the valuable commodities.

There is an important role for geochemistry in the exploration workflow. Especially, for very broad distribution of trace elements around IOCG deposits, and these can be used to recognize 'halos' within mineral systems, also for deposits beneath thick surface sediment formation (Fabris et al., 2015).

In geochemistry the stochastic dependences between different major and trace elements occurring in deposit are often analyzed, because the relations could enable us to understand and to explain some unexpected phenomena or emerge some valuable rules. For example in the ores of high Fe grade there is often low Ti with variable Cu, Au, Ag as well as REE or in allanites-Ce the REE concentration is inversely proportional to the Ca contents (Zhao and Zhou, 2011; Barton, 2014). Ag contents in multistage deposits (skarn, massive sulfides, and black shale) abrupt increase in later low-temperature assemblages regardless of deposit type (Gas'kov, 2017). Letnikova with her co-workers (2011) used geochemical correlations of different oxides to reconstruct the geodynamic processes of forming deposits in Tuva-Mongolian Massif. In the placer gold deposits in the East of Siberian Platform with increasing of Au fineness the Ag content is decreased and Cu has an increasing tendency (Nikiforova et al., 2018).

Though the IOCG Sin Quyen deposit has been investigated by several scientists, but they have principally focused on the geological structure, ore crystallization ages and occurrence of the specific minerals (Ta, 1975;

McLean, 2001; Ishihara et al., 2011; Gas'kov et al., 2012; Li and Zhou, 2018; Pieczonka et al., 2019). The correlation coefficients between some elements in IOCG Sin Quyen deposit were also estimated by Gas'kov et al. (2012), but the correlations were not interpreted or very weakly considered. In this paper we intend to present some interesting characteristic correlations between chalcophile elements (Cu, Ag, Au, Pb, Bi, Te, and Zn), the siderophile elements (Fe, Co, Ni), the lithophile elements as well as between the radioactive elements (Th, U) and major ore elements Cu, Au, Ag and REE. Though in the IOCG Sin Quyen deposit the sulfur and iron currying minerals are dominating but there is no correlation between these elements and others even with Cu, the phenomena will be also considered.

Study area

The Sin Quyen IOCG deposit is located in the Lao Cai province, 300 km north-western from Hanoi and one km from the Red River, which is the natural boundary with China (Fig.1). The coordinate of the deposit is 22^{o} 37' 20'' of latitude and 103^{o} 48' 00'' of longitude with 200ha of area. From the geological point of view, the deposit is within the Red River zone in the west of the Fanxipan belt. The Fanxipan belt divides the North Vietnam into the South China block and the Indochina block, and trending in the NW-SE direction with near 300 km long in the Vietnam territory. The Fanxipan belt is composed of high-grade metamorphic complex zone. The Red River zone is composed of the Suoi Chieng and Sin Quyen formations (Fig.2). The Suoi Chieng formation with near 600 m thick is built principally from the Proterozoic terrigenous sediments and granitic gneiss, biotite-amphibole gneiss and biotite schits. The Suoi Chieng suit is covered conformably by the Sin Quyen formation with 1200 m round of thick. From the facies point of view the Sin Quyen formation is divided into lower and upper units. In the lower unit there is gneiss composing of the biotite, muscovite and graphite quartz, while the composition of the upper unit is similar to the lower one, but without graphite. The Sin Quyen formation is intruded by several mafic intrusive dikes or lenses and is overlain conformable by the Cambro-Ordovician Cam Duong sediments (McLean, 2001; Gas'kov et al., 2012; Ishihara et al., 2011).

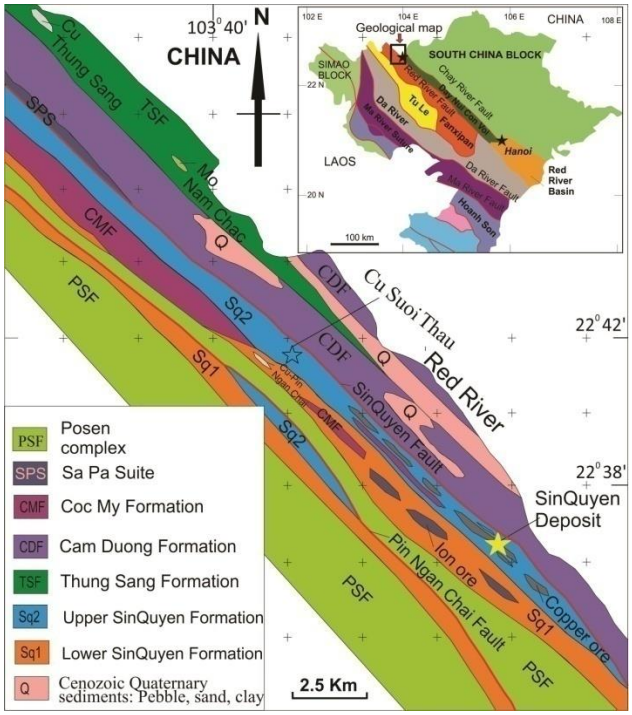

Fig. 1. Localization of the Sin Quyen deposit on the geological sketch of the North Vietnam

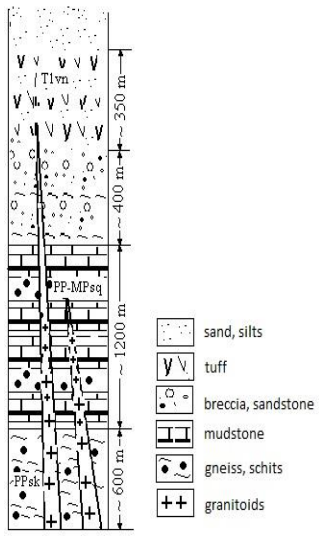

Fig. 2. Schematic illustration of the rock formation in the Sin Quyen region

Fig. 3. Cross section of the ore body (photo 2015, looking NW direction)

The ore bodies of the IOCG Sin Quyen deposit principally are hosted in the Sin Quyen formation, they occur as the lenses with several tens meters thick and up to few hundred meters long, trending NW-SE and dipping near vertically (70-90°) (Fig. 3). The major ore minerals are Au-, Ag-rich copper and iron sulfides (chalcopyrite, pyrite, and pyrrhotite) and iron oxides (magnetite, hematite). The average grade of Cu, LREE and Au is equal to 0.9 wt.%, 0.7 wt.% and 0.44 ppm respectively. With the Cu grade of 0.9 wt.% and the maximum depth of the ore body occurrence 350 m b.s.l, the Cu calculated resource of the IOCG Sin Quyen deposit amounts to near 90 Mt (McLean, 2001; Pham et al., 2015). The deposit has an uncommon ore composition and divided horizontally into two parts (Fig. 4). The first is wide spread in the central and eastern area, in this part the main ore minerals are chalcopyrite, pyrrhotite and pyrite, the minerals contribute near 90% ore composition. The second part predominates in the western, where the major minerals are magnetite, pyrite, chalcopyrite and pyrrhotite contributing from a few percent up to 50% of ore (McLean, 2001; Gas'kov et al., 2012). Due to the occurrence of the large fractures system, the oxidized zone is clearly observed in the upper part near 100 m of depth below the earth surface (Fig. 5) (Pieczonka et al., 2019).

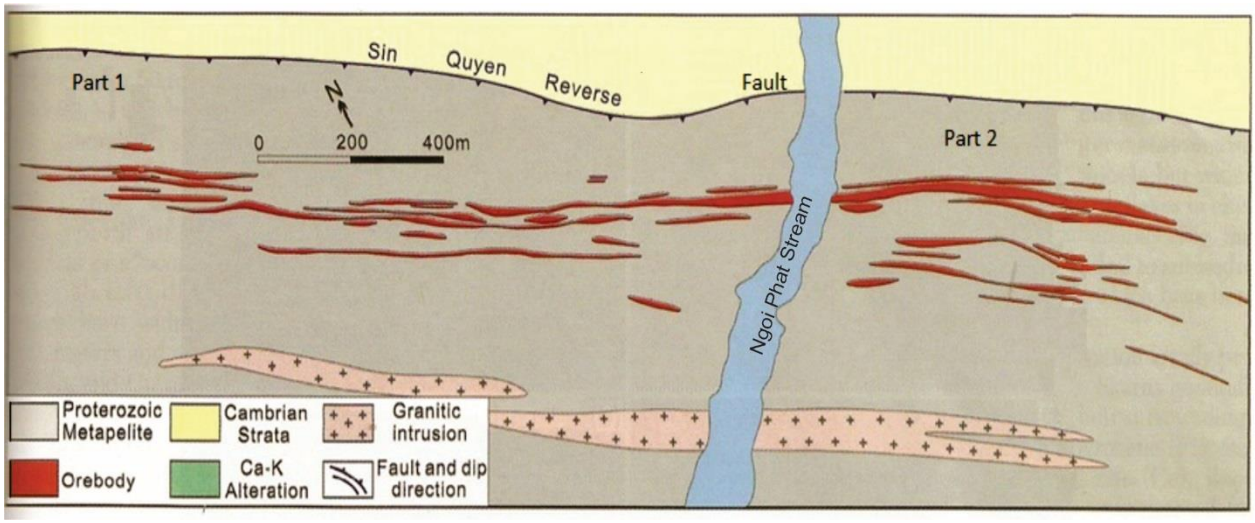

Fig. 4. Modified Geological sketch of Sing Quyen deposit after Ta (1975)

According to Li et al. (2017), in the deposit region there were four principal mineralization stages: (i) the paragenetic sequence including with the sodic alteration, which was happened in the Proterozoic epoch; (ii) the calcic-potassic alteration and associated Fe-REE-(U) mineralization lasted in the Neoproterozoic (841 to

836 Ma); (iii) Cu-Au mineralization, the third stage probable happened at 500 Ma (Pieczonka et al., 2015, 2019) and the fourth stage was connected with the metamorphism occurred at the 30 Ma and the sulfide-(quartz-carbonate) veins were mostly established. The mineralization of the Sin Quyen deposit basically falls within the age range of the Neoproterozoic igneous rocks (740 – 860 Ma) (Li et al., 2017).

Fig. 5. View of weathered zone (photo, 2014)

Materials and methods

On November 2014 at the IOCG Sin Quyen deposit, 50 solid samples from massive ores, host rocks, reservoir sediments, Cu - and Fe-concentrates and from waste dumps were collected. The localization of the sampling places is shown in figure 6.

All the collected samples were analyzed by optical microscope at AGH University of Science and Technology (AGH UST). Based on the results of the microscope analyze, 39 samples were selected for the chemical compositions and natural radionuclides analyzed. The chemical composition was analyzed at Bureau Veritas Mineral Laboratories in Canada using the method assigned as AQ251 and NAA. The sample of 0.5 g was digested in Aqua Regia at 90 °C followed by an ICP-MS. The analytical methods in detailed, detection limits and uncertainties can be downloaded from the ACME Laboratories website at www.acmelab.com. Analytical uncertainties are typically 5% for most analysed elements. Detection limit for REEs varies from 0.02 up to 0.5 ppm. For the natural radionuclide determination, the sample was milled until the grains became less than 2 mm, then it was dried in an oven at 120 °C for 24 h to ensure that moisture was completely removed, then weighted and packed in an aluminum cylindrical beaker and sealed to prevent the escape of radon. The weighed and tightly sealed samples were left for at least 21 days to reach secular equilibrium between ^{226}Ra and ^{222}Rn as well as its daughters (mostly ^{214}Bi and ^{214}Pb). The activity concentration was determined using a semiconductor HPGe detector (Canberra GX4020) with 42% relative efficiency. The energy resolution of the spectrometer at the line 1333 keV (^{60}Co) is near 2 keV. As standard samples, reference materials RG produced by the International Atomic Energy Agency (IAEA) were used. Samples were measured in cylindrical beaker with 48 cm^3 of volume (sample diameter 70 mm, height 12.5 mm) placed directly on the detector. The measurement time of samples amounted near 50 h. A detail description of the methodology is presented by Jodlowski and Kalita (2010).

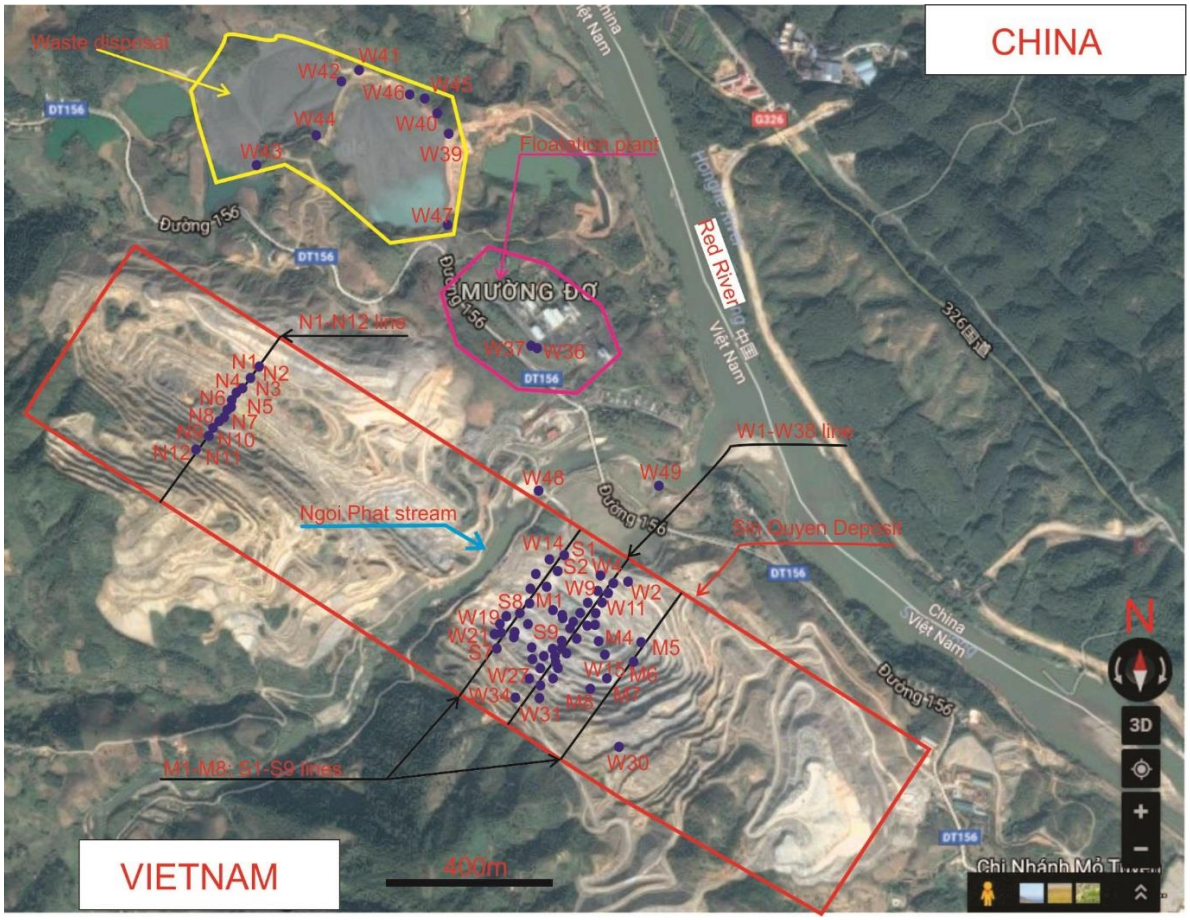

Fig. 6. Sampling localization

Results and discussions

The analyzed chemical concentration of the most measured elements in the samples varied in the broad ranges (Table 1). The ratio of the maximum to minimum concentrations in the ore samples of the major elements range from 10^2 to 10^5 (ppm). The Fe concentration in the ore ranges from near 1% to 40%. The maximum concentration of Fe in the massive ore is on the level of the Fe concentrate (samples W18, W37), Cu content ranges from near 0.004% up to 11% (samples W31a and S4), the Au and Ag average concentrations are higher than that of earth crust about 10^5 and 10^3 fold and equal to 1662 and 1163 ppb respectively. Gold and silver are randomly occurring as an electrum mineral in a vein forms (Fig. 7a). The economic or anomalous gold is common characteristic for IOCG deposits in the World (Zhu, 2016). In the deposit REE bearing minerals are allanites occurring in disseminated manner (Fig. 7b). The total concentration of rare earth elements (TREE) varies from 22 ppm to about 2500 ppm with 700 ppm of average. The concentration of light rare earth element (LREE) is significantly higher than that of heavy rare earth elements (HREE), their average ratio (LREE/HREE) equal to 70. The sulfur grade ranges from 0.06 to 7.5% with 2.04% of average. This value is near 10^3 times higher than the earth crust average concentration. The average U and Th concentrations are 84 and 13 ppm and higher than the earth average concentration by 24 and 1.4 fold respectively, so the uranium is the main radioactive element in the deposit. The general reasons for uranium enrichment in IOCG deposit could include the hydrothermal fluids (Hitzman and Valenta, 2005).

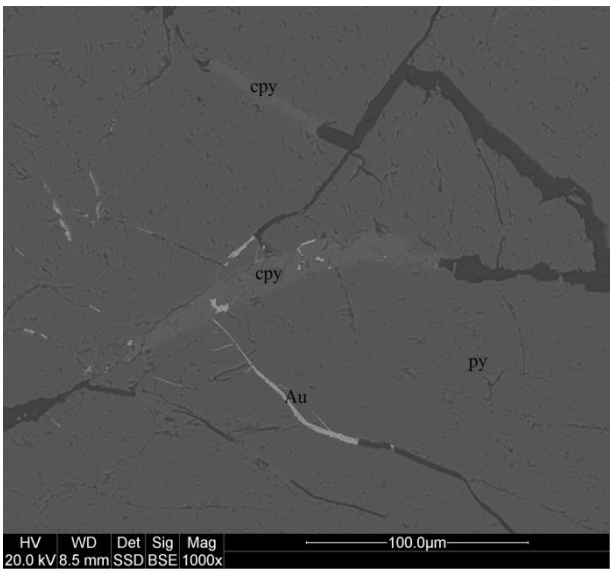

Fig. 7a. BSE image showing position of electrum (Au) in relation to pyrite (py) and chalcopyrite (cpy). Reflected light

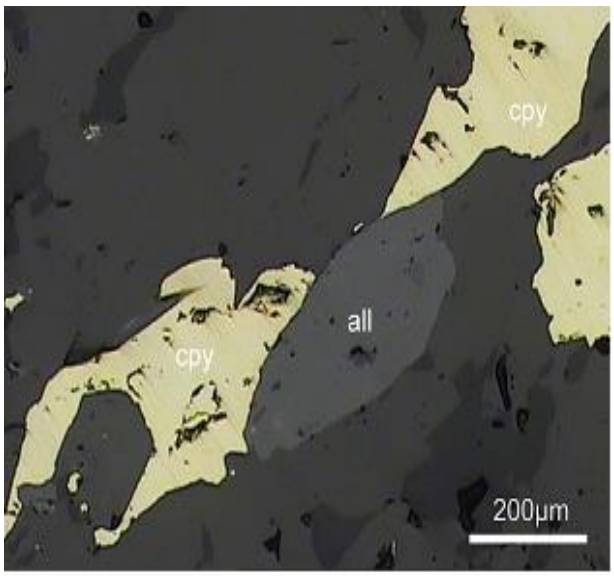

Fig. 7b. Intergrowth of allanite (all) with chalcopyrite (cpy). Reflected light

Using the data in the table 1, the correlations between different elements were performed, and their coefficients are summarized in table 2. All the values of correlation coefficients (R) higher than 0.5 are mark in bold. According to the statistics background and excluding the relations between sulfur and iron with other elements, we consider only the strong relations, it means that the relations, which R is higher than 0.7. The correlation coefficients between Cu and Ag, Te, Bi, Pb and Au are higher than 0.7 and equal to 0.94, 0.94, 0.90, 0.82 and 0.73 respectively (Tab. 2, and Fig. 8a– 8e). Cu, Au, and Ag belong to the chalcophile elements group, which naturally prefer to bond with sulfur to form the resist compounds (Palyanova et al., 2018; Gas'kov, 2017). Au and Ag often occur together with pyrite, chalcopyrite and pyrrhotite (Fig. 7a). These elements are in a strong correlation (R= 0.79, Fig. 9) indicating high similarity in their geochemical properties.

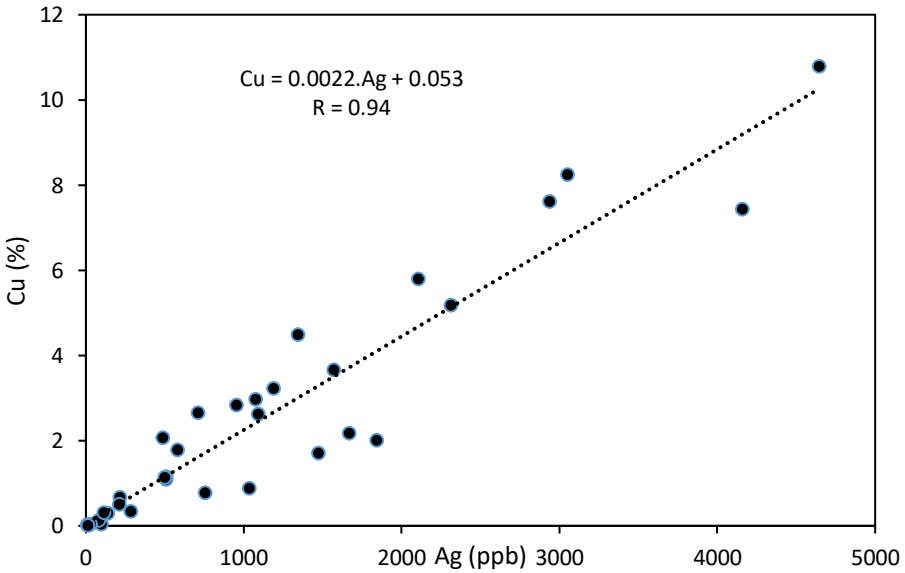

Fig. 8a. The correlation between Cu and Ag concentration

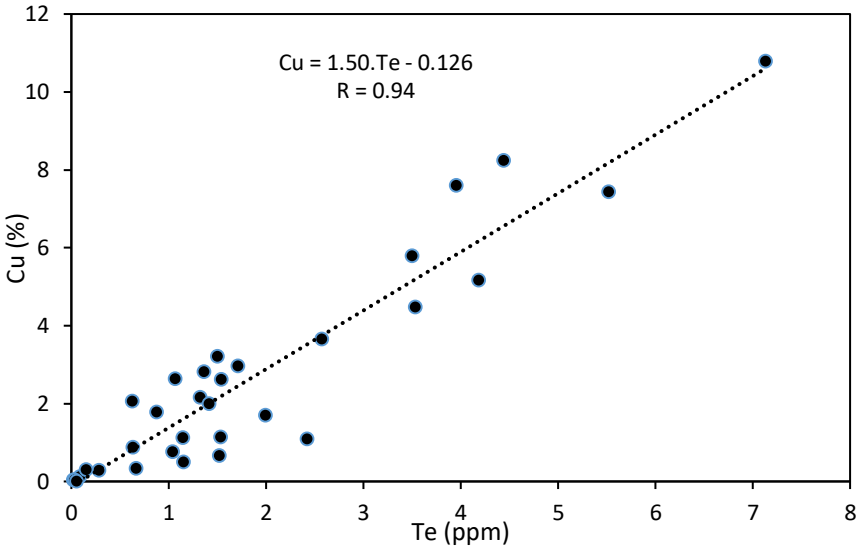

Fig. 8b. The correlation between Cu and Te concentration

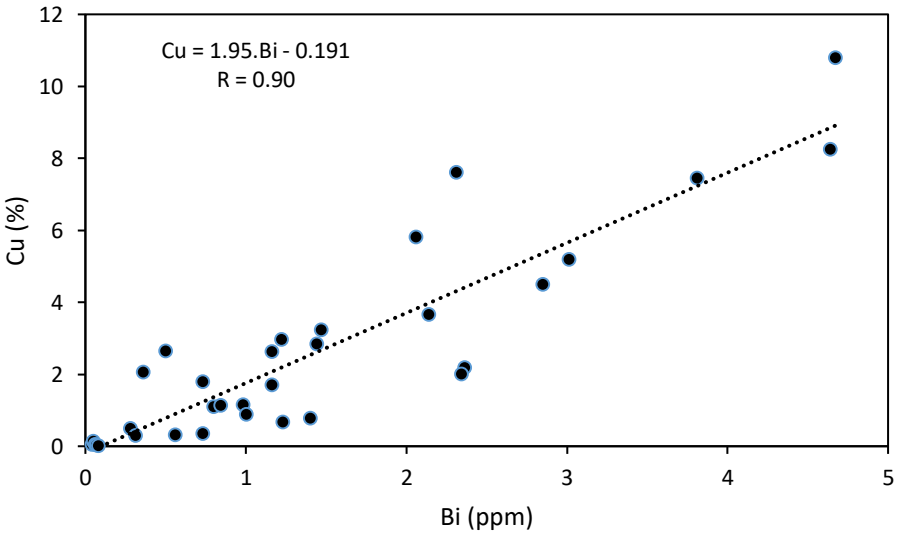

Fig. 8c. The correlation between Cu and Bi concentration

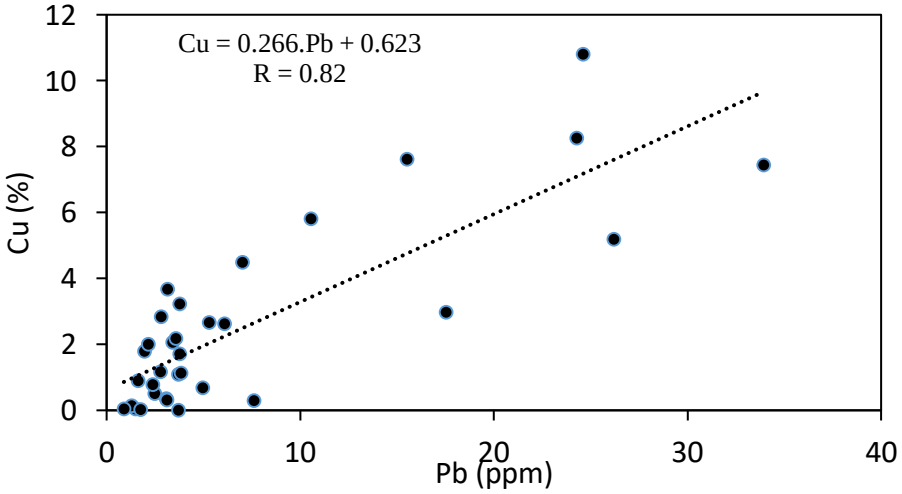

Fig. 8d. The correlation between Cu and Pb concentration

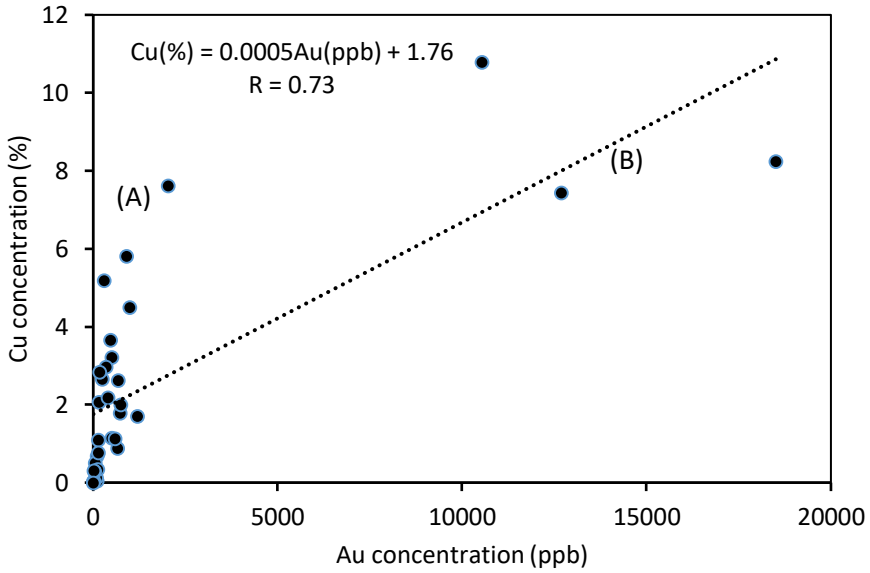

Fig. 8e. The correlation between Cu and Au concentration

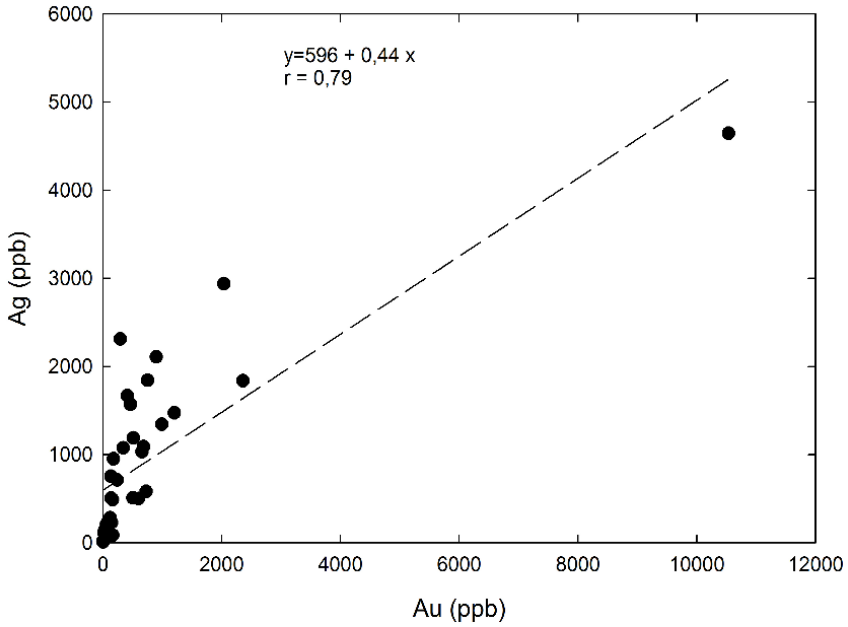

Fig. 9. Plot of relation between Au and Ag

Au-Ag alloy often commonly occurs in micro-vein form in gold and copper minerals with trace elements of Hg (Knight and Leitch, 2001; Gas'kov et al., 2001). The correlation Cu-Au is lower than Cu-Ag (compare Fig. 8a and Fig. 8e), indicating a part of Au formed separately as native form, and other part of Au crystalized together with Ag and Cu. In other hand silver is more affine to sulfur than to gold and tend to enter sulfide minerals (Gas'kov, 2017). These processes are depended on the content of Au, Ag and Cu in the hydrothermal fluid, crystallization temperature and sulfur fugacity (Palyanova et al., 2018; Gas'kov, 2017). The significantly high concentrations of Au (> 10 000 ppb) and Ag (>4000 ppb) are observed only in the samples of the Cu-Fe massive ore, suggesting electrum intergrowth with sulfide minerals mainly in breccias ores. The high correlation coefficients are observed also for Cu-Te (R= 0.94) and Cu-Bi (0.90) (Tab. 2 and Fig. 8b, 8c). In intrusive fluid high tellurium can bind silver and gold and forms as silver and gold tellurides (Gas'kov, 2017). In the Sin Quyen copper deposit Te and Bi are trace elements with 1.9 ppm and 1.4 ppm of average concentration respectively. These concentrations are comparable with that in the other IOCG deposits in the World (Mikulski, 2014). Generally presence of Te and Bi in IOCG deposit is related to the Au-Ag-Bi-Te-Pb mineral association as arsenopyrite and polymetallic sulfite (Mikulski, 2014). In the deposit, intergrowth of

bismuthinite (Bi_2S_3) with chalcopyrite (Fig. 10), indicating that these minerals crystalized at the similar temperature.

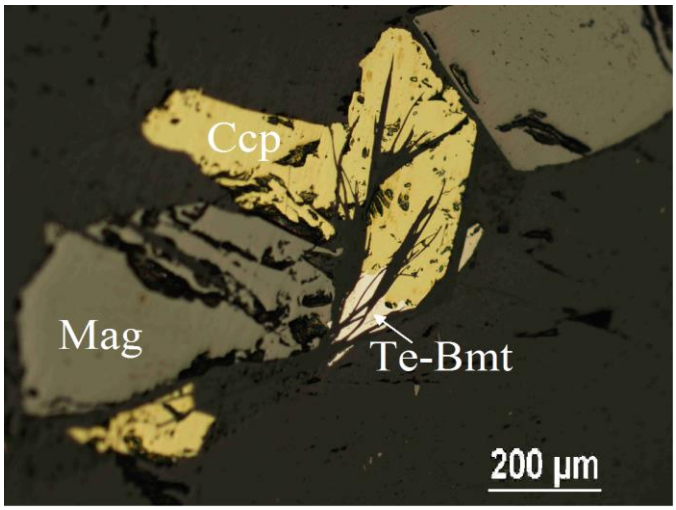

Fig. 10. Te-Bismuthinite (Te-Bmt) with chalcopyrite (Ccp) in reflected light

In the weathered zone bismuthinite reacts with water and is transform into the bismite (Bi_2O_3) or bismutite $Bi_2(CO_3)O_2$ (Gruszczyk, 1984). Figure 8d presents the relation between Cu and Pb with R= 0.82, Pb is also specific chalcophile elements. The Pb, Te and Bi concentrations are in order of several ppm (Tab. 1), therefore the elements in the IOCG deposits are regarded as the impurity and not classified as co-product elements (Barton, 2014).

Generally uranium and thorium minerals such as uraninite, thorite, thorianite and allanite are often present in IOCG deposits. Although low grade enough, the world' uranium greatest resource is in the IOCG Olympic Dam deposit in Australia (9.2 Gt @ 270 ppm U), the smaller uranium resources occur in other IOCG assemblages including the Kangdian metallogenic province in SW China, Qiaoxiahala deposit in Jungar region, NW China, Ayazmant skarn deposit in Ayvalik (Balikesir), Turkey and the others (Hitzman and Valenta, 2005; Chen et al., 2015; Li et al., 2014; Oyman, 2010). The main bearing uranium in the Sin Quyen deposit is uraninite. This mineral often exists as an intergrowth with chalcopyrite, magnetite, and allanite in the Cu-Fe massive ore (Fig. 11). Owing the high uranium concentration the Sin Quyen deposit was discovered by radiometric survey (Ta, 1975). The correlation coefficient of the Cu-U amounts to 0.78 (Tab. 2). Similar correlation coefficient of Cu-U was observed in the case of the Polish copper mines in Lubin mining district (Niewodniczański, 1981; Piestrzyński, 1989).

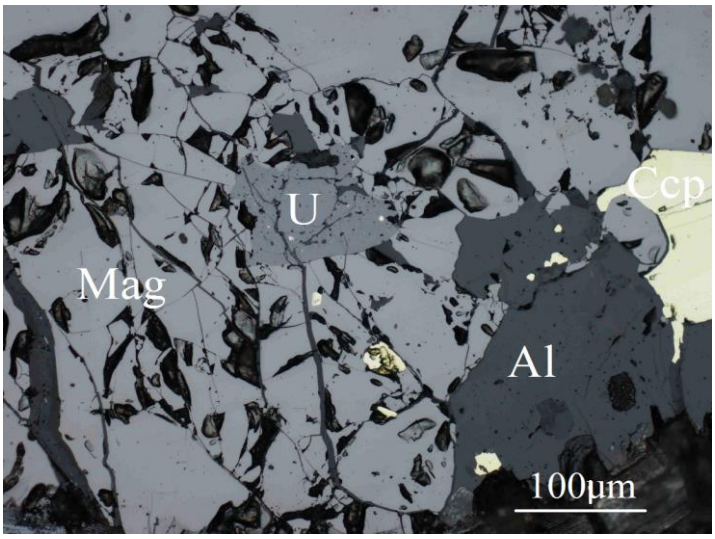

Fig. 11. Intergrowth of uraninite (U) with magnetite (Mag), chalcopyrite (Ccp) and allanite (Al). Reflected light

Iron is the most basic element in the studied deposit, its concentration varies from near 1 percent up to above 40 percent. However, the coefficients of the correlation between this element and other elements were relatively low (≤0.6). The low correlation coefficients of Fe with other elements in the study deposit were also reported by Gas'kov et al. (2012). The weak correlation of Fe probably is connected with the geochemical property of this element. In nature Fe can occur at the state of 2+ or 3+, and rarely 0. Depending on the redox and chemical condition, Fe can bond with sulfur or oxygen and form sulfate or sulfide or oxide compounds. In Sin Quyen deposit there are many Fe-bearing minerals, such as rock forming and chalcopyrite, bornite, pyrrhotite, pyrite and magnetite indicating that in the deposit there were inhomogeneous fluid. Several crystallization stages accompanied with different geological and crystallization conditions have been recognized in the deposit (Gas'kov et al., 2012; Pieczonka et al., 2015; Li et. al., 2018). Additionally there are some zones characterized with different major minerals (Gas'kov et al., 2012; Pieczonka et al., 2015). Using the archival data reported by Ta (1975), the plot of the relation between two principal elements Cu and Fe in the deposit is shown in figure 12.

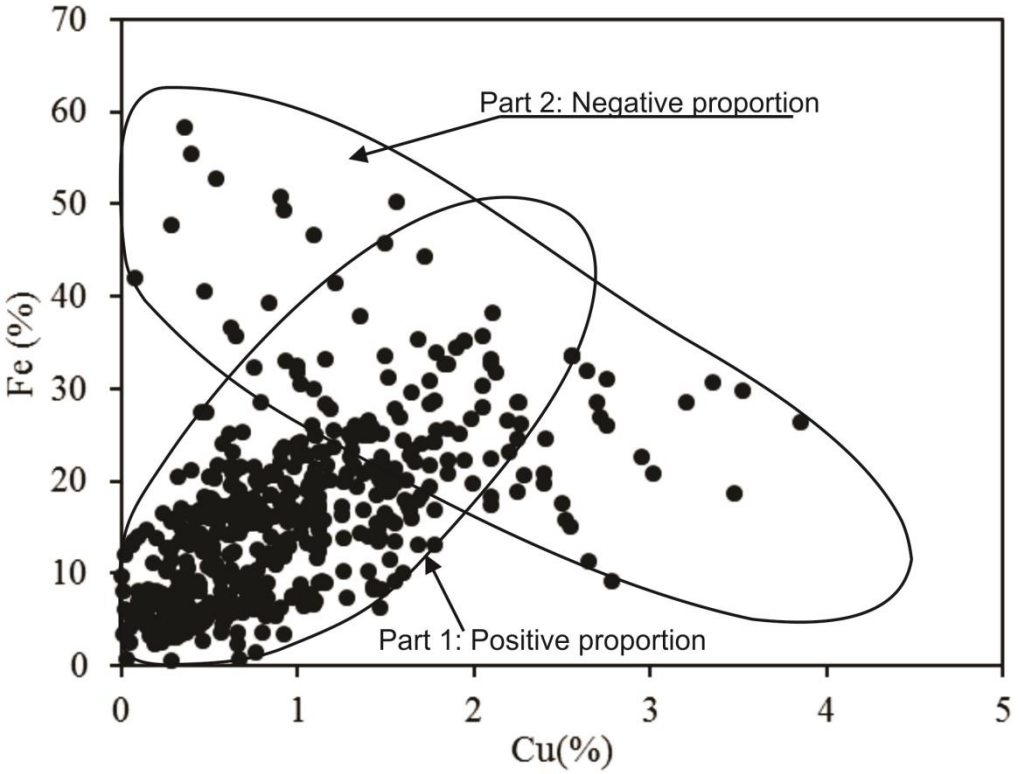

Fig. 12.The plot of relation between Fe and Cu concentration (the data were taken from the paper published by Ta (1975))

The Cu-Fe plot (Fig.12) can be divided into two parts. In the first part there are relatively low concentrations of both Fe and Cu and characterized by the linearly increasing of Fe with Cu. The second part Fe is dominating and decreasing with Cu. Two mentioned parts could be corresponded to the two types of ores described by Gas'kov et al. (2012). The samples with positive correlation belong to the first zone and the most of samples with negative correlation are within the second deposit part.

Co and Ni are the typical siderophile elements and often occur in the sulfoarsenides or with Fe in pyrrhotite or pyrite, but their grades in IOCG deposit are rarely exceed 100 ppm (Barton, 2014; Gas'kov, 2017). In the Sin Quyen deposit the concentrations of these elements range from a few ppm up to 300 ppm (Tab. 1). The maximum concentrations are far below of the economic grade of Co, Ni deposit. The correlation coefficient is equal to 0.9 (Tab. 2) and the view of the plot of the Ni-Co couple is shown on figure 13a. The high correlation coefficient reflects the close mineralogical association of Co and Ni and the comparable concentration ranges of these elements in the study deposit. The correlation coefficient of the Fe-Co pair amounts only to 0.62 (Fig. 13b), but the value of the correlation coefficient of the Co-S pair is equal to 0.83 (Tab. 2, and Fig. 13c), suggesting that Co mostly occurring as substitution at the sulfides.

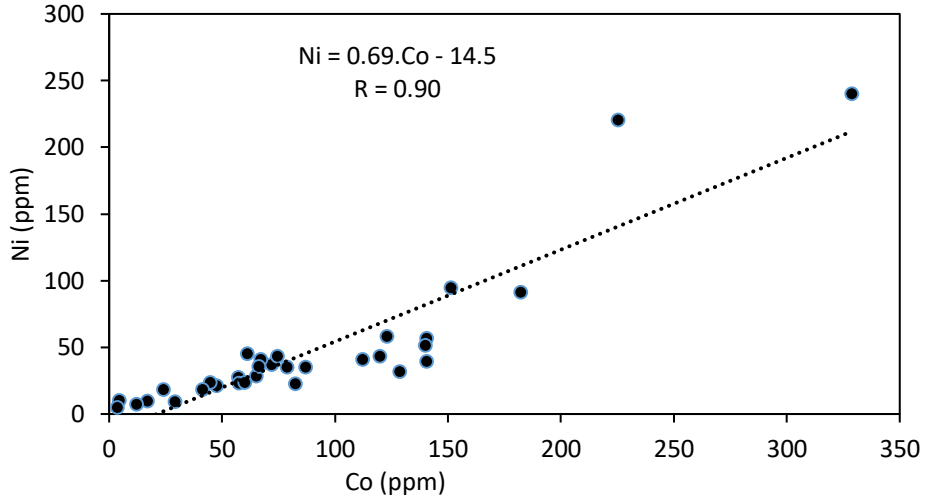

Fig. 13a. Plot of relation between Co and Ni

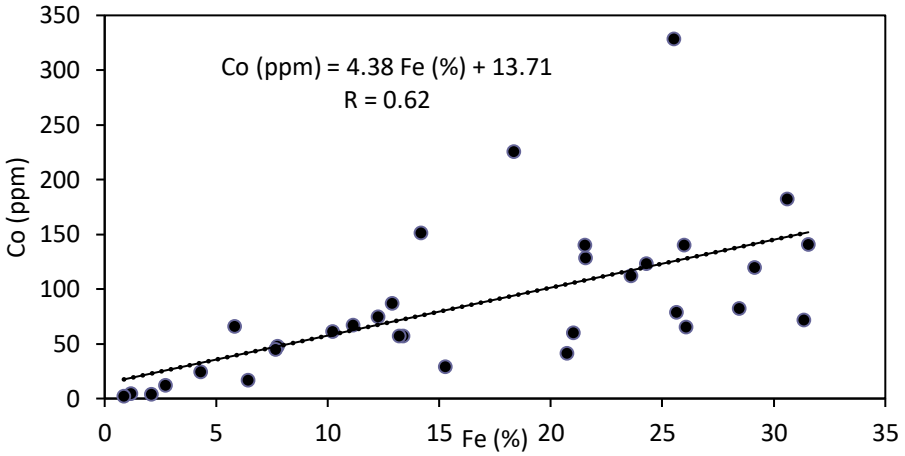

Fig. 13b. Plot of relation between Fe and Co

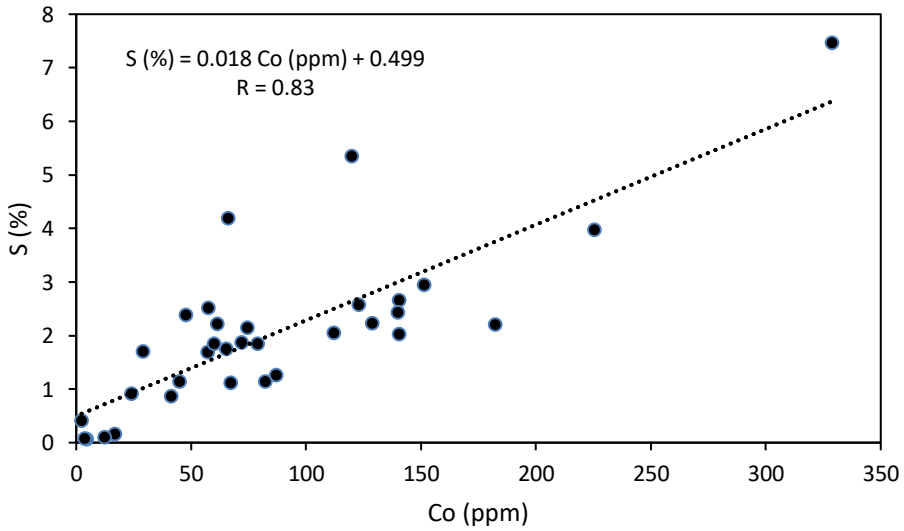

Fig. 13c. Plot of relation between Co and S

Natural radioactive elements often play very important roles in the geophysical survey especially for deposits rich in these elements. The average activity concentrations of ^{40}K, ^{226}Ra and ^{232}Th in the Sin Quyen deposit were recorded at 496, 691 and 59 Bq/kg respectively. The correlation coefficients of the pairs: U-Cu, U-Pb,

U-Au, U-Ag, U- Bi and U-Te amount to 0.78, 0.97, 0.78, 0.81, 0.75, and 0.78 respectively (Table. 2 and Fig. 14a-14f). Such high correlation enable us to determine the mentioned nonradioactive elements in the solid samples through measurements of uranium and save significantly the analyze costs. In the Sin Quyen deposit, the principal radioactive element is uranium (Nguyen et al., 2016), the main mineral bearing uranium is uraninite, its presence is often observed within the copper massive ores (Ishihara et al., 2011; Pieczonka et al., 2015). The high correlation coefficient of U-Pb (R = 0.97, Fig. 14b) probably is connected with the ^{206}Pb isotope (the last isotope in the uranium series), which principally contributes in the content of the whole of lead in the deposit. The good correlation between U and Au, Ag, Bi and Te suggests the minerals currying these elements principally crystalized at the similar temperatures. According to Gas'kov (2008) the crystallization temperatures of the mentioned elements bearing minerals: uraninite, tellurobismuthite, sulfoaresenides varied from 200 to 75 °C.

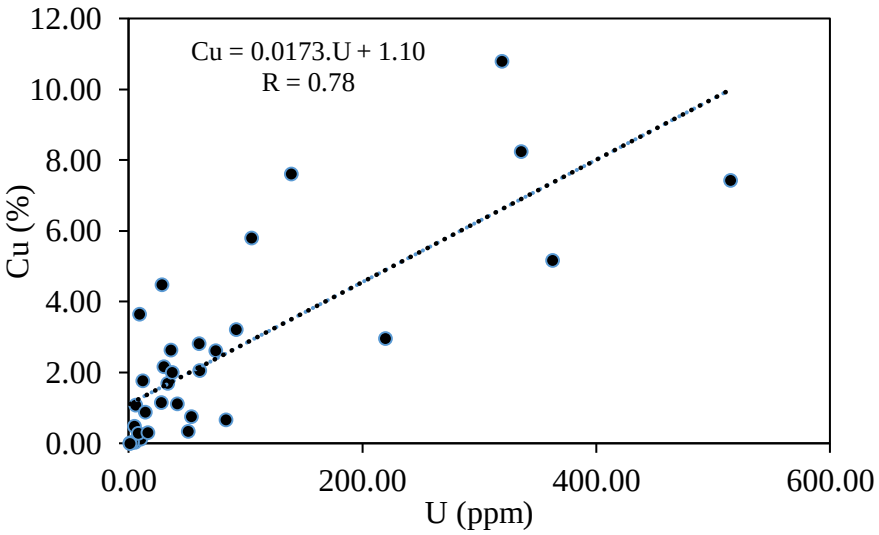

Fig. 14 a. The correlation between U and Cu concentration

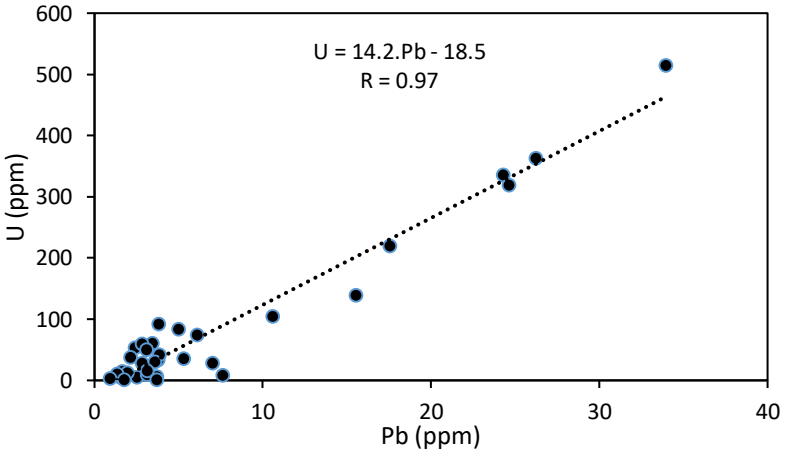

Fig. 14b.The correlation between U and Pb concentration

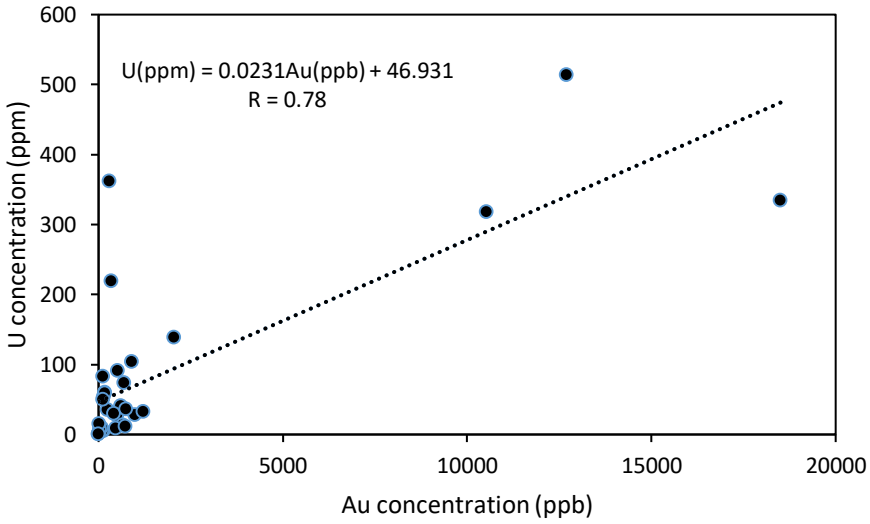

Fig. 14c. The correlation between U and Au concentration

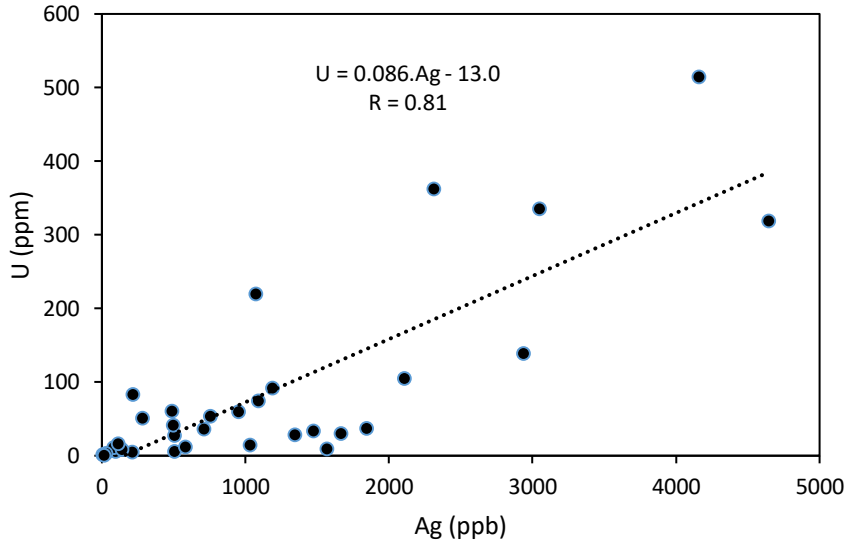

Fig. 14d. The correlation between U and Ag concentration

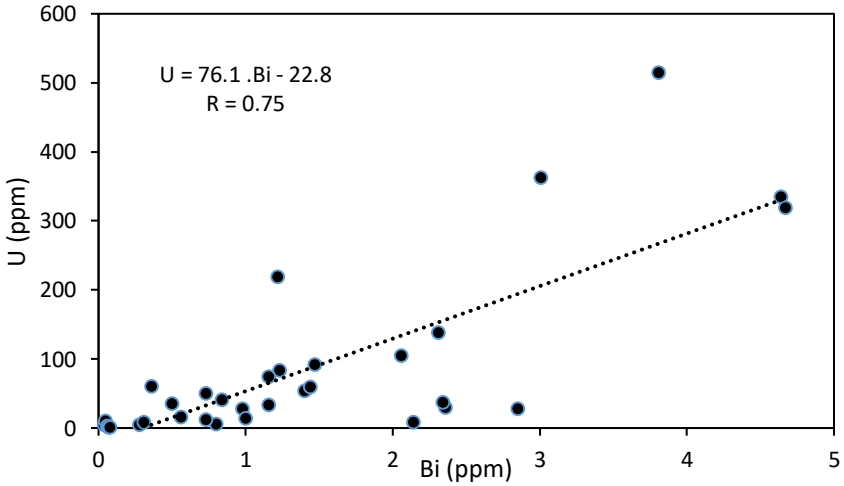

Fig. 14e. The correlation between U and Bi concentration

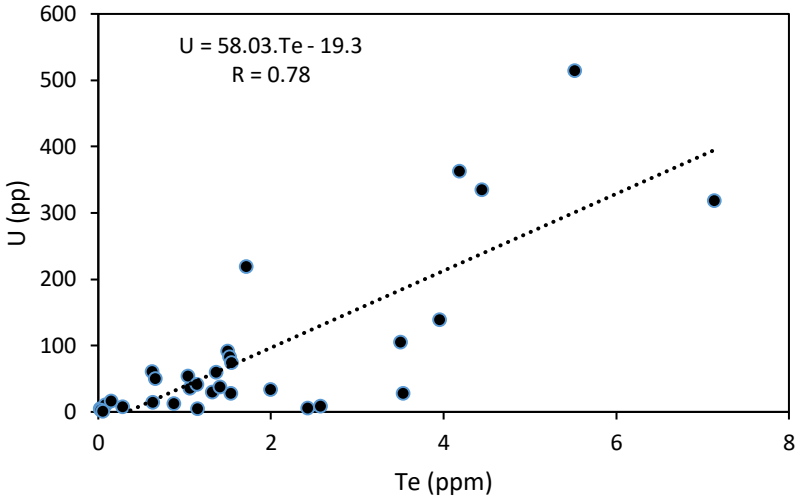

Fig. 14f Relation between U and Te

The reservoir of the rare earth elements (REE) is on the third place after Fe and Cu in the Sin Quyen deposit (Ta, 1975; McLean, 2001; Ishihara et al., 2011; Gas'kov et al., 2012; Li and Zhou, 2018). The main REE bearing mineral is allanite (Fig. 11). Usually it occurs either at low concentrations, 1-2 vol%, or very rarely as a major mineral. The average content of allanites in the ore is on the level of 0.98 wt% (Pieczonka, et al., 2015). There is no correlation with other element observed, suggesting allanites were formed separately from the sulfide and oxide ores (Gas'kov et al., 2012).

In the deposit there are two groups of allanites (Fig. 15a–15d), the outer rim is younger. Different tints in the grey color show mosaic textures of allanite crystals. This can be interpreted either as a change in the fluid composition during crystallization, or changes in the composition during Na-alteration (Li and Zhou, 2018). The older allanite group is with REE content from 23 to 27%, and the younger with 19 to 23% and higher amounts of Al_2O_3, CaO and SiO_2 (McLean, 2011; Pieczonka, et al., 2015). The allanites can be classified as La-Ce-ferriallanite, and a variety with low Y, U and Th. The difference of the mentioned two groups could be resulted from the alteration processes occurring in the study deposit.

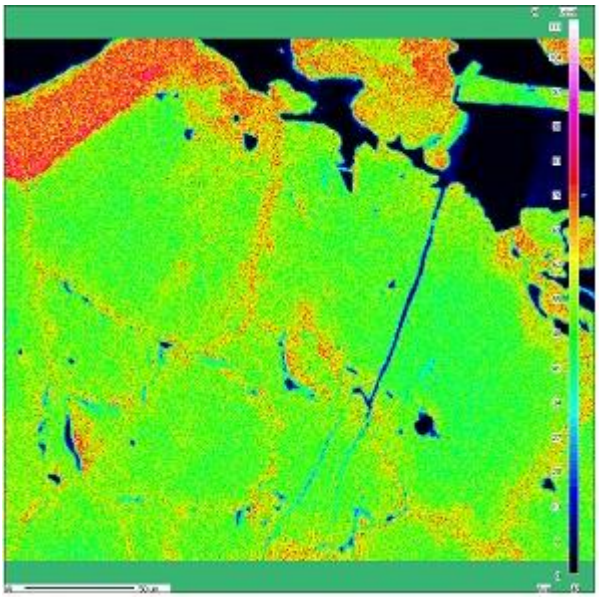

Fig.15a. Contour map of Al in allanites

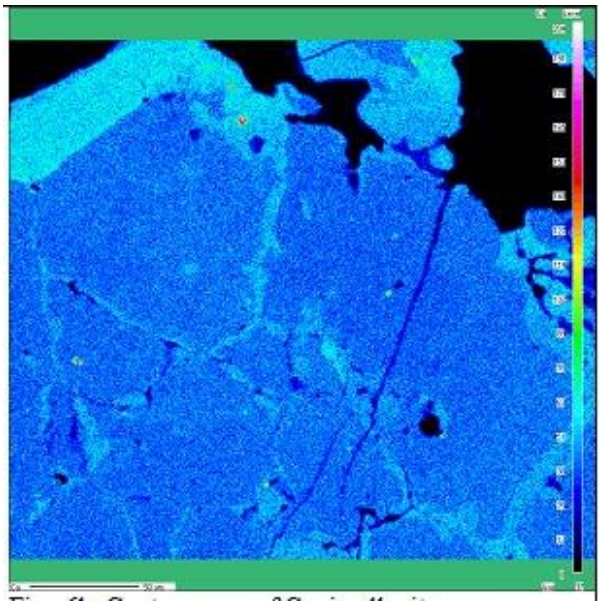

Fig. 15b. Contour map of Ca in allanites

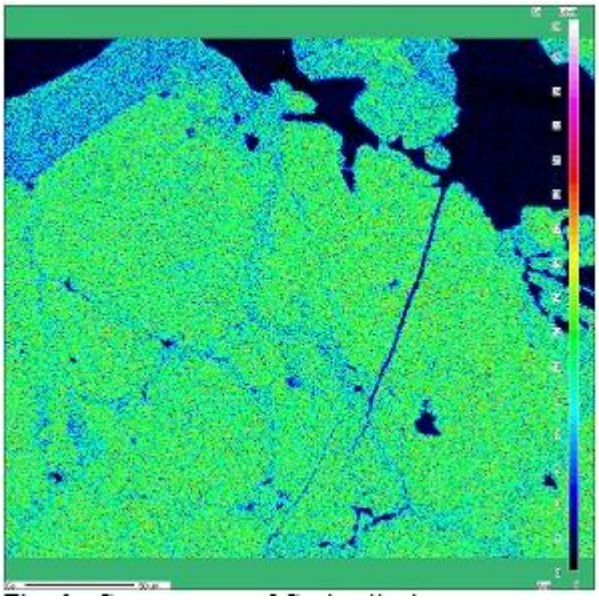

Fig.15c. Contour map of Ce in allanites

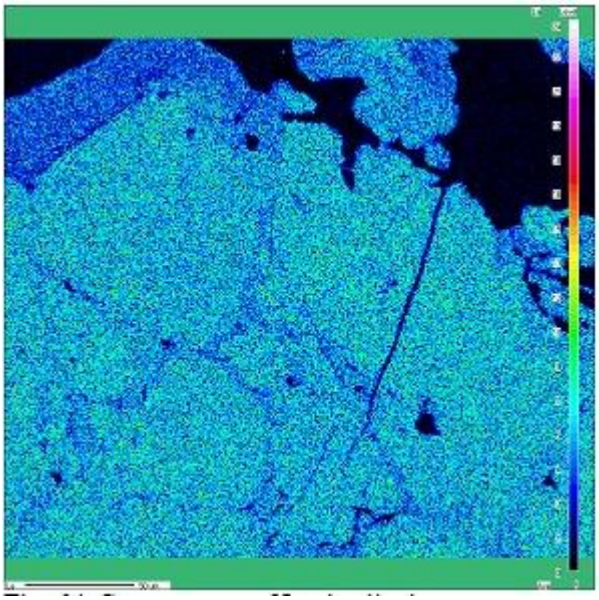

Fig.15d Contour map of La in allanites

Sulfur is very interesting element in IOCG deposit, its average concentration in the deposit amounts to 2.04 % (Tab. 2). The sulfur minerals are dominating in the deposit, but excluding relation between S and Co, the correlation coefficients of the relation between sulfur and other major, minor as well as trace elements are below 0.5 (Tab. 2). The relation between S and other elements is the first time considered in this paper. In general the crystallization of the sulfur minerals requires a relatively oxidized (SO_4^{2-}> H_2S) and low in total sulfur (Barton, 2014). In IOCG deposit sulfur occurs in different sulfides (pyrite, chalcopyrite, pyrrhotite). Due to high chemical active, sulfur is easily bound with different elements to form different minerals. Therefore the total sulfur is spread into many compounds and no clear correlation between this elements with the others. The suggestion was tested by the correlation between sulfur and the sum of Fe and Cu (Fe+Cu), which correlation coefficient R is equal to 0.56 (Fig. 16), the value is far higher than that of the correlation between Cu and other single element.

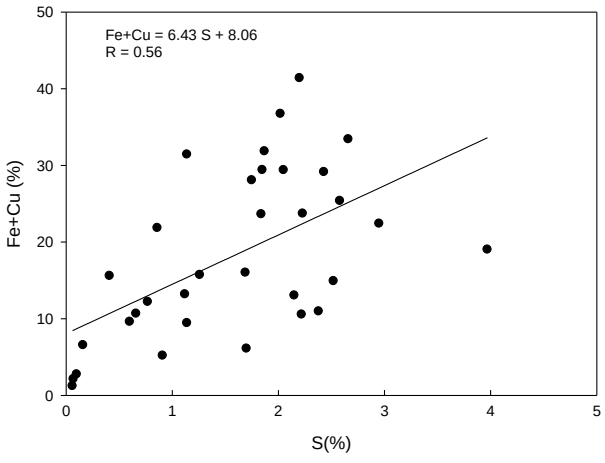

Fig. 16. Plot of relation between S and (Cu+Fe)

Conclusions

Generally the statistic analyze is very important in the most practice matters. In the Earth sciences the statistic calculus is named as geostatistics, which consist in the probability and statistic correlation between different parameters of the geological objects. The authors of this paper attempted to deal with the relations between the major, minor and trace elements focusing on the strong correlations and inspected relations. Based on the presented results and calculated correlation coefficients as well as geological and geochemical analyze, some conclusions are emerged as follow:

1. The strong correlations between the elements belong to the chalcophile group, to which Cu, Ag, Au, Pb, Bi and Te belong. The correlation coefficients between the elements in this group are higher than 0.7 and not sensitive on the ranges of the element concentrations.
2. The correlation between Fe and other elements even with Co, and Ni, which belong to the siderophile group is very weak or not observed. The phenomena can be consequence of the chemistry property of iron and geological as well as geochemical conjunctures in the IOCG Sin Quyen deposit. It worth adding there is strong correlation between Co and Ni, the reason is that both elements not only have close mineralogical association but also their grade ranges are comparable in the deposit.
3. Between Cu and Fe there are clearly two relations, one is positive proportion and the second is negative proportion, the two relations probably are connected with the two horizontally separated parts of the Sin Quyen deposit.
4. There are strong correlation between uranium and several elements, such as: Cu, Ag, Au, Pb, Bi and Te. The strong correlation between U and Cu, Ag and Au can be resulted from the crystalization of uraninite together with the chalcopyrite and electrum minerals in the deposit.
5. There is very weak correlation or no between REE and other elements, the fact can be connected with allanite was formed separately from other minerals (Li et al., 2017).
6. No correlation between sulfur and major and minor or trace elements, the phenomena are resulted from the very chemical activity of this element. Sulfur is sensitive on the crystallization condition (temperature, pressure) and redox and easily reacts with many elements to form crystalized compounds, therefore there is no strong correlation between sulfur and other single element.

Acknowledgment

The work was made in the scope of the bilateral cooperation between Hanoi University of Mining and Geology (UMG) and AGH University of Science and Technology No.01/2012/HD-HTQTSP and foundered from UST-AGH Krakow for financial support, grant no 11.11.140.161 and 11.11.140.645.

References

Barton, M.D., 2014. Iron oxide (-Cu-Au-REE-P-Ag-U-Co) systems. Elsevier, 515-537.

Chen, W.T., Zhou M.F., Gao, J.F., Hu, R., 2015. Geochemistry of magnetite from Proterozoic Fe-Cu deposits in the Kangdianmetallogenic province, SW China. Mineralium Deposita 50, 795-809.

Fabris, A., Wielen, S., Keeping, T., Gordon, G., 2015. Geochemical footprints of IOCG deposits beneath thick cover: insights from the Olimpic Cu-Au province, South Australia. Conf. Materials of 27th International Applied Geochemistry Symposium (IAGS). Tuscon, 20-24.

Gandhi, S.S., 2003. An overview of the Fe oxide-Cu-Au deposits and related deposit types. CIM Montreal 2003 Mining Industry Conference and Exhibition, Canadian Institute of Mining, Technical Paper, CD-ROM.

Gas'kov, I.V., 2008. New data on the correlation of skarn and gold mineralization at the Tardan deposit (Northeastern Tuva). Russian Geology and Geophysics 49 (12), 923–931.

Gas'kov, I.V., 2017. Major impurity elements in native gold and their association with gold mineralization setting in deposits of Asian folded areas. Russian Geology and Geophysics 58, 1080–1092.

Gas'kov, I.V., Distanov, E.G., Kovalev, K.R., Akimtsev, V.A., 2001. Gold and silver in polymetallic deposits of northwestern Rudny Altai. Russian Geology and Geophysics 42 (6), 850–867.

Gas'kov, I.V., Tran,T.A., Tran, T.H., Pham T.D.,Nevolko, P.A., Pham, N.C., 2012. The Sin Quyen Cu-Fe-Au-REE deposit (northern Vietnam) composition and formation conditions. Russian Geology and Geophysics 53, 442–456.

Groves, D.I., Bierlein, F.P., Meinert, L.D., Hitzman, M.W., 2010. Iron oxide copper-gold (IOCG) deposits through Earth history: Implications for origin, lithospheric setting, and distinction from other epigenetic iron oxide deposits. Economic Geology 105, 641-654.

Gruszczyk, H., 1984. Science of ores [in Polish]. WG, Warszawa.

Hitzman, M.W., Oreskes, N., Einaudi, M.T., 1992. Geological characteristics and tectonic setting of Proterozoic iron oxide (Cu–U–Au-REE) deposit. Precambrian Res. 58, 241–287.

Hitzman, M.W., Valenta, R.K., 2005. Uranium in iron oxide-copper-gold (IOCG) systems. Economic Geology 100, 1657-1661.

Ishihara, S., Hideo, H., Mihoko, N.C., Pham, T.D., Pham, T.A., Tran, T.H., 2011. Mineralogical and chemicalcharacteristics of the allanite-rich copper and iron ores from the Sin Quyen mine, northern Vietnam. Bulletin of the Geological Survey of Japan 62 (5/6), 197 - 209.

Ivan, K.B., Thomas, K., Radostina, A., Colin, J.A., 2002. Morphogenesis and composition of native gold in the Chelopech volcanic-hosted Au-Cu epithermal deposit, Srednogorie zone, Bulgaria. Mineralium Deposita 37, 614-629.

Jodlowski, P., Kalita, S., 2010. Gamma-Ray Spectrometry Laboratory for high-precision measurements of radionuclide concentrations in environmental samples. Nukleonika 55 (2), 143−148.

Knight, J., Leitch, C.H.B., 2001. Phase relations in the system Au–Cu–Ag at low temperatures, based on natural assemblages. The Canadian Mineralogist 39, 889-905.

Letnikova, E.F., Veshcheva, S.V., Proshenkin, A.I., Kuznetsov, A.B., 2011. Neoproterozoic terrigenous deposits of the Tuva–Mongolian massif: geochemical correlation, source lands, and geodynamic reconstruction. Russian Geology and Geophysics 52, 1662–1671.

Li, Q., Zhang, Z., Geng, X., Li, C., Liu, F., Chai, F., Yang, F, 2014. Geology and geochemistry of the Qiaoxiahala Fe-Cu-Au deposit, Junggar region, northwest China. Ore Geology Review 57, 462-481.

Li, X.C., Zhou, M.F., 2018. The nature and origin of hydrothermal REE mineralization in the Sin Quyen deposit, northwestern Vietnam. Economic Geology 113 (3), 645-673.

Li, X.C., Zhou, M.F., Chen, W.T., Zhao, X.F., Tran, M.D., 2017. Uranium-lead dating of hydrothermal zircon and monazite from the Sin Quyen Fe-Cu-REE-Au-(U) deposit, northwestern Vietnam. Mineralium Deposita 53(3), 399-416.

McLean, R.N., 2001. The Sin Quyen iron oxide–copper–gold–rare earth oxide mineralization of North Vietnam, in: T. M. Porter (Ed.), Hydrothermal Iron Oxide and Copper–Gold Related Deposits: A Global Perspective. PGC Publishing 2, 293–301.

Mikulski, S.Z., 2014. The occurrence of tellurium and bismuth in the gold-bearing polymetallic sulfide ores in the Sudetes (SW Poland), [in Polish with abstract in English]. Mineral Resources Management 30 (2), 15-34,

Nguyen, D.C., Le, K.P., Jodłowski, P., Pieczonka, J., Piestrzyński, A., Duong, H.V., Nowak, J., 2016. Natural Radioactivity at the Sin Quyen iron oxide copper gold deposit in North Vietnam, Acta Geophysica 64 (6), 2305-2321**.**

Niewodniczański, J., 1981. A radiometric analysis of nonradioactive ores [in Polish with summary in English]. Scien. Bull. The Stanisław Staszic Academy of Mininig and Metallurgy, No 303 "Mathematics-Physics-Chemistry". Cracow, Poland.

Nikiforova, Z.S., Gerasimov, B.B., Glushkova, E.G., Kazhenkina, A.G., 2018. Indicative features of placer gold for the prediction of the formation types of gold deposits (*east of the Siberian Platform*). Russian Geology and Geophysics 59, 1318–1329.

Oyman, T., 2010. Geochemistry, mineralogy and genesis of the Ayazmant Fe-Cu skarn deposit in Ayvalik, (Balikesir), Turkey. Ore Geology Review 37, 175-201.

Palyanova, G.A., Murzin, V.V., Zhuravkova, T.V., Varlamov, D.A., 2018. Au-Cu-Ag mineralization in rodingite and nephritoids of the Agardag ultramafic massif (southern Tuva, Russia). Russian Geology and Geophysics 59, 238–256.

Pham, Q.D., 2015. Exploration report on no.3 and no.7 ore bodies of the Sin Quyen deposit, Lao Cai province [in Vietnamese]. Archival Magazine of National Geology Department of Vietnam.

Pieczonka, J., Piestrzyński, A., Le, P.K., Nguyen, C.D., Jodłowski, P., 2015. Rare Earth, Radioactive and selected elements in the iron oxide copper gold Sin Quyen deposit in North Vietnam. In: Viet-Pol 2015 second international conference on scientific research cooperation between Vietnam and Poland in Earth Sciences, 331-353.

Pieczonka, J., Nguyen, C.D., Piestrzyński, A., Le, P.K., 2019. Timing of ore mineralization using minerals and U-Pb dating in IOCG Sin Quyen deposit, North Vietnam. Geological Quarterly (in Press).

Piestrzyński, A., 1989. Uranium and thorium in copper ore deposits on the Fore-Sudetic Monocline (SW Poland). Mieralogia Polonica 20 (1), 41-53.

Requia, K., Fontboté, L., 2000. The Salobo iron-oxide copper-gold deposit, Carajas, Northern Brazil, in Porter, T.M., ed., Hydrothermal iron oxide copper-gold and related deposits: A global perspective. PGC Publishing, Adelaide.

Requia, K., Stein, H., Fontboté, L., Chiaradia, M., 2003. Re-Os and Pb-Pb geochronology of the Archean Salobo iron oxide copper-gold deposit, Carajas mineral province, northern Brazil. Mineralium Deposita 38, 727-738.

Ta, V.D., 1975. Report of geological surveys and their results performed at the IOCG Sin Quyen deposit in Lao Cai, North Vietnam [in Vietnamese]. Main Department of Geology of Vietnam.

Zhao, X.F., Zhou, M.F., 2011. Fe-Cu deposits in the Kangdian region, SW China a Proterozoic IOCG (iron-oxide-copper-gold) metallogenic province. Mineralium Deposita, 46 731-747.

Zhu, Z., 2016. Gold in iron oxide copper-gold deposits – A review. Ore Geology Review 72, 37-42.

Caption of Tables

Caption of Figures

Table 1. Bulk chemical composition of the samples from Sin Quyen deposit (ACME lab.)

	Fe	Mn	Co	Ni	Au	Cu	Zn	Ag	Pb	Ga	Ge	S	Marks
Units	%	ppm	ppm	ppm	ppb	ppm	ppm	ppb	ppm	ppm	ppm	%	
MDL	0.01	1	0.1	0.1	0.2	0.01	0.1	2	0.01	0.1	0.1	0.02	
M1	25.52	274	328.7	240.3	502.6	11539	40.9	508	2.79	4	0.3	7.46	Ep-Am rock, Cu-Fe ore
M2	7.74	308	47.6	21.4	511.1	32225	85.9	1188	3.79	5.5	0.4	2.38	Ep-Am rock, Cu ore
M3	18.34	512	225.3	220.7	107.6	6751	21.6	216	4.98	5.1	0.7	3.97	Ep-Am rock
M4	29.14	226	119.7	43.4	991.8	44900	67.9	1344	7.01	11.4	0.6	5.35	massive Cu-Fe ore
M5	28.45	528	82.3	22.7	343.5	29700	50.3	1075	17.53	17.8	0.8	1.14	Cu-Fe ore
M6	13.36	499	57.2	27.4	237.5	26524	187.1	711	5.29	10.7	0.5	1.69	Bt-Am rock,Cu ore
M7	31.35	305	71.8	37	59.3	4972	38.8	211	2.49	14.7	0.9	1.87	massive Fe ore
M8	24.28	1028	123	58.5	138	10914	137.8	506	3.7	22.1	0.7	2.58	massive Cu-Fe ore
N1	4.31	330	24.1	18.7	657.3	8811	33.3	1034	1.64	10.7	0.4	0.91	Ep-Qtz-Pl rock
N2	1.18	137	4.5	10.3	102.3	404	9.1	98	1.5	4	0.1	0.06	Carbonate-Quartz rock
N3	12.26	791	74.5	43.6	132.3	7695	48.4	754	2.38	22.9	0.7	2.15	skarn
N4	13.21	583	57.3	23.1	1204.4	16976	173.5	1475	3.77	15.9	0.6	2.52	Bt-Am rock, Cu ore
N5	25.62	605	78.8	35.4	462.9	37861	118.2	1569	3.13	16.4	0.7	1.85	Bt-Ep rock, Cu-Fe ore
N6	25.97	332	140.4	57.1	12687.5	74400	195.9	4159	33.92	13.8	0.6	2.66	Cu-Fe ore
N7	7.66	414	44.8	23.9	727.7	17769	48.4	581	1.94	10.6	0.4	1.14	Cb-Qtz rock, Cu ore
N8	11.13	399	67.2	40.9	161.9	20614	59.1	488	3.41	15	0.3	1.12	Bt-Qtz-Amp rock Cu ore
N9	6.43	627	16.8	9.7	88.9	1302	26.4	83	1.31	9.1	0.4	0.16	Amphibolite
N10	12.89	449	86.9	35.2	175.9	28309	96.4	952	2.8	23.1	0.3	1.26	Amphibolite Cu ore
N11	14.17	417	151.2	94.7	18503.7	82400	145.8	3050	24.27	11.7	0.3	2.95	Massive Cu ore
N12	20.72	332	41.2	18.5	598.1	11258	51.8	498	3.84	15.5	0.5	0.86	Ep-Am rock, Cu-Fe ore
S1	10.21	521	61.2	45.6	121.2	3447	91.6	283	3.07	13.5	0.4	2.22	Bt-Am schist
S2	21.55	240	128.6	32	407.8	21709	82.6	1668	3.56	15.9	0.7	2.23	Cu-Fe ore
S3	31.55	255	140.5	39.4	294.7	51806	182.2	2311	26.21	13.4	0.7	2.02	Massive Cu-Fe ore
S4	30.6	114	182.2	91.3	10531.2	107878	152.2	4646	24.6	9.7	0.6	2.2	Massive Cu-Fe ore
S5	21.02	272	60	24	681.2	26150	77.9	1090	6.09	9.6	0.5	1.84	Cu-Fe ore
S6	21.53	244	139.9	51.7	2038.6	76083	109.9	2939	15.53	7.7	0.5	2.43	Massive Cu-Fe ore
S7	2.08	156	3.6	4.9	10.4	394	12.6	30	0.89	6.2	0.1	0.07	Carbonate-Quartz rock
S8	26.06	334	65.2	28.6	750.1	19988	43.8	1844	2.14	18.6	0.7	1.75	Massive Cu-Fe ore
S9	23.59	173	112.1	41	897.7	58040	104	2107	10.56	8.1	0.4	2.05	Cu-Fe ore
W-15	2.73	1085	12.2	7.3	3.1	186	32.5	8	1.76	-	-	0.1	ore, open pit
W-18	>40	319	99.2	41.4	2358.2	>10000	88.3	1836	5.46	-	-	4.19	massive ore
W-25	5.81	758	66.1	35.7	28.6	2935	34.1	139	7.61	-	-	1.7	epid-amph rock
W-31	15.28	1479	29.1	9.4	16.9	3067	57.7	113	3.11	-	-	0.41	skarn
W-31a	0.86	1264	2.3	<0.1	1.6	39	33.3	14	3.7	-	-	<0.02	skarn with garnet
Min	0.86	114	2.3	4.9	1.6	39	9.1	8	0.89	4	0.1	0.06	
Max	40	1479	328.7	240.3	18504	107900	196	4646	33.92	23.1	0.9	7.46	
Average	17.2	480	86.6	46.5	1662.81	25670	80.6	1163	7.23	12.5	0.51	2.04	
Std. Dev	10.4	324	68.2	51.7	4033.42	27465	53.45	1168	8.37	5.38	0.20	1.53	
W-36	35.0	236	183	91.6	6489.7	>10000	580.1	30909	40.8	-	-	8.33	Cu-concentrate
W-37	>40	356	135.3	84.8	148.2	998	28	230	3.56	-	-	3.62	Fe-concentrate
W-39	10.6	880	46.6	26.2	68.8	555	64.3	136	4.97	-	-	0.66	Waste I

W-40	9.57	792	36.6	24.1	67.3	386	52.2	86	4.2	-	-	0.6	Waste II
W-44	12.17	711	30.9	20.1	166.7	335	42.3	86	5.31	-	-	0.77	Waste out from tailing

Table 1. Continue

Elements / Units	Sn Ppm	Te ppm	Tl ppm	Bi ppm	Cd ppm	U ppm	Th ppm	Sr ppm	V ppm	Cs ppm	Cr ppm	Ti %	Marks
MDL	0.1	0.02	0.02	0.02	0.01	0.1	0.1	0.5	2	0.5	0.5	0.001	
M1	17.8	1.53	0.06	0.98	0.18	27.9	11.3	8.5	28	0.22	16	0.025	Ep-Am rock, Cu-Fe ore
M2	25.3	1.5	0.06	1.47	0.39	91.9	30.5	48	50	0.38	8.1	0.078	Ep-Am rock, Cu ore
M3	67.3	1.52	0.02	1.23	0.1	83.5	28.6	20.9	44	0.8	18.8	0.072	Ep-Am rock
M4	19.6	3.53	0.21	2.85	0.45	28.4	7.6	11.3	90	3.34	19.3	0.083	massive Cu-Fe ore
M5	14.8	1.71	0.57	1.22	0.23	219.7	12.6	102.1	104	6.72	20	0.141	Cu-Fe ore
M6	22.7	1.06	0.34	0.5	0.7	36.1	12.6	19.3	50	3.14	26.8	0.098	Bt-Am rock,Cu ore
M7	21.1	1.15	0.03	0.28	0.12	5	3.7	12.3	37	0.41	5	0.017	massive Fe ore
M8	17.1	2.42	0.18	0.8	0.32	5.9	5.7	32.2	69	5.5	9.6	0.058	massive Cu-Fe ore
N1	17.7	0.63	0.56	1	0.12	14.5	31.5	13.2	41	10.85	23.4	0.254	Ep-Qtz-Pl rock
N2	3.5	0.02	0.12	0.04	0.03	5.5	6.5	17	10	2.38	12.6	0.069	Carbonate-Quartz rock
N3	18.1	1.04	1.28	1.4	0.1	53.9	19.2	26.8	99	26.32	50.3	0.241	skarn
N4	27.1	1.99	0.87	1.16	1.46	33.7	23.4	9.7	65	16.93	36.7	0.148	Bt-Am rock, Cu ore
N5	21.3	2.57	0.72	2.14	0.68	9.1	9.9	16.3	112	5.58	30	0.191	Bt-Ep rock, Cu-Fe ore
N6	37.9	5.52	0.46	3.81	1.58	514.7	11.8	27.7	103	2.6	20	0.113	Cu-Fe ore
N7	20.2	0.87	0.23	0.73	0.25	12.3	5.2	16.4	87	3.03	26.9	0.116	Cb-Qtz rock, Cu ore
N8	8.8	0.62	0.62	0.36	0.26	60.6	7.4	6.6	67	8	117	0.167	Bt-Qtz-Amp rock Cu ore
N9	21.6	0.08	0.07	0.05	0.06	10.7	25.9	20.6	50	1.36	18.6	0.087	Amphibolite
N10	9.3	1.36	1.1	1.44	0.49	60.2	22.2	5.7	104	21.27	46.2	0.266	Amphibolite Cu ore
N11	20.8	4.44	0.42	4.64	1.02	335.6	10.1	17.8	78	2.27	32.5	0.061	Massive Cu ore
N12	5.6	1.14	0.88	0.84	0.15	41.6	14.3	8.3	87	14.41	63.8	0.266	Ep-Am rock, Cu-Fe ore
S1	18.5	0.66	1.88	0.73	0.21	50.8	9.1	8.5	48	48.69	25.7	0.199	Bt-Am schist
S2	10.4	1.32	0.72	2.36	0.72	30.3	13	17.7	92	11.22	4	0.116	Cu-Fe ore
S3	36.3	4.18	0.38	3.01	1.17	362.8	3	8.7	92	6.52	11.6	0.099	Massive Cu-Fe ore
S4	24.1	7.13	0.08	4.67	0.7	319.2	13.1	25	81	1.01	1.9	0.045	Massive Cu-Fe ore
S5	14	1.54	0.21	1.16	0.38	74.6	19.6	22.2	73	3.61	28.4	0.111	Cu-Fe ore
S6	18.5	3.95	0.22	2.31	0.57	139	22.5	43.7	67	1.51	15.8	0.074	Massive Cu-Fe ore
S7	1	0.03	0.06	0.06	0.01	3.3	12.8	6.7	15	0.63	6.9	0.015	Carbonate-Quartz rock
S8	10.7	1.41	0.53	2.34	0.11	37.4	42.4	16.2	138	5.71	25.9	0.17	Massive Cu-Fe ore
S9	13.9	3.5	0.19	2.06	0.67	105	20.6	21.4	61	2.32	19.1	0.077	Cu-Fe ore
W-15	-	0.05	-	0.07	0.06	1.17	2.2	90.8	51	-	-	0.283	ore, open pit
W-18	-	3.6	-	2.58	0.41	56.51	2.9	11.4	123	-	-	0.075	massive ore
W-25	-	0.28	-	0.31	0.11	8.35	1.4	128	50	-	-	0.303	epid-amph rock
W-31	-	0.15	-	0.56	0.03	16.31	0.9	22.3	74	-	-	0.268	skarn
W-31a	-	<0.02	-	0.08	0.07	0.98	0.5	98.2	<2	-	-	0.012	skarn with garnet
Min	1	0.02	0.02	0.04	0.01	0.98	0.5	5.7	10	0.22	1.9	0.012	
Max	67.3	7.13	1.88	4.67	1.58	514.7	42.4	128	138	48.69	117	0.303	
Average	19.5	1.9	0.5	1.4	0.4	84.0	13.6	28.3	70.9	7.5	25.5	0.1	
Std Dev.	12.4	1.7	0.4	1.3	0.4	122.6	10.2	30.3	30.2	10.3	22.5	0.1	
W-36	-	4.91	-	5.39	3.31	20.56	2.2	52.1	62	-	-	0.06	Cu-concentrate

W-37	-	0.64	-	1.28	0.1	22.7	2.9	13.1	219	-	-	0.125	Fe-concentrate
W-39	-	1.04	-	1.74	0.14	32.56	12.2	51	89	-	-	0.245	Waste I
W-40	-	0.86	-	1.32	0.14	30.64	8.7	45.1	83	-	-	0.256	Waste II
W-44	-	0.38	-	1.68	0.06	62.43	11.3	46	85	-	-	0.225	Waste out from tailing

Table 1. Continue

Elements	Ba	Mg	Al	Na	K	Ca	Nb	Rb	Sc	Y	LREE	HREE	TREE	Marks
Units	ppm	%	%	%	%	%	ppm	ppm	ppm	ppm	ppm	ppm	ppm	
MDL	0.5	0.01	0.01	0	0.01	0.01	0.02	0.01	0.02	0.01	0.01	0.01	0.01	
M1	7	0.14	0.55	0.09	0.14	1.09	0.74	2.5	1.1	6.65	487	3.8	490	Ep-Am rock, Cu-Fe ore
M2	6.7	0.34	0.95	0.12	0.19	2.16	1.5	4.9	3.2	20.41	2245	11.1	2256	Ep-Am rock, Cu ore
M3	4	0.03	0.59	0.01	0.02	4.12	2.49	3.8	1.8	81.39	1077	44.4	1122	Ep-Am rock
M4	13.4	0.25	0.56	0.06	0.25	0.59	2.55	24.5	2	9.49	704	4.7	709	massive Cu-Fe ore
M5	170	1.71	2.03	0.02	2.3	2.58	2.03	115	3.3	17.2	1378	10.3	1388	Cu-Fe ore
M6	130	0.53	1.63	0.08	1.15	1.4	1.27	56.8	2.6	9.12	622	5.1	627	Bt-Am rock,Cu ore
M7	10.9	0.14	0.68	0.11	0.13	0.92	0.33	4.3	1.4	4.24	145	2.3	148	massive Fe ore
M8	88.2	0.69	2.13	0.11	0.48	2.37	0.28	58.2	3.7	8.32	214	4.8	219	massive Cu-Fe ore
N1	197	2.77	2.82	0.07	2.81	0.57	0.26	112	7.5	46.83	1466	25.9	1492	Ep-Qtz-Pl rock
N2	53.8	0.61	0.88	0.16	0.58	1.51	0.26	24.4	3.7	38.6	575	19.7	595	Carbonate-Quartz rock
N3	247	3.39	4.81	0.01	3.87	1.99	1.2	194.2	5.5	11.97	961	6.0	967	skarn
N4	128	0.59	2.16	0.17	1.11	1.29	1.14	107.7	6.2	14.87	672	7.8	680	Bt-Am rock, Cu ore
N5	155	1.52	2.28	0.03	2.21	1.04	1.47	114.4	11.9	13.33	832	7.2	840	Bt-Ep rock, Cu-Fe ore
N6	80.6	0.48	1.08	0.04	0.62	1.02	0.72	39.1	2.4	17.85	626	10.2	636	Cu-Fe ore
N7	112	0.91	1.99	0.2	0.76	1.46	0.37	37.8	3.4	9.57	184	4.8	189	Cb-Qtz rock, Cu ore
N8	241	2.64	3.79	0.05	2.55	0.3	0.34	112	6.1	7.43	126	4.1	130	Bt-Qtz-Amp rock Cu ore
N9	21.3	1.26	2.16	0.34	0.26	2.82	0.27	10.3	4.1	13.91	173	6.8	179	Amphibolite
N10	284	5.43	5.9	0.01	4.11	0.32	1.11	178.5	5.7	8.2	154	4.5	159	Amphibolite Cu ore
N11	34.2	1.5	2.42	0.07	0.3	1.51	0.43	20.4	2.5	10.17	292	6.1	298	Massive Cu ore
N12	364	1.12	3.22	0.05	2.97	0.38	0.98	150	3.6	7.09	475	3.3	478	Ep-Am rock, Cu-Fe ore
S1	159	3.35	3.57	0.03	3.3	0.46	0.58	294.2	2.4	4.99	421	2.5	424	Bt-Am schist
S2	104	2.57	2.19	0.03	2.84	0.49	1.73	170	2.2	10.4	656	4.9	661	Cu-Fe ore
S3	57.6	0.5	1	0.04	0.79	0.6	1.55	59	1.6	11.42	177	6.4	184	Massive Cu-Fe ore
S4	12.9	0.25	0.3	0.02	0.17	0.98	1.41	9.4	1.1	30.56	1694	15.8	1710	Massive Cu-Fe ore
S5	74.8	0.45	1.14	0.1	0.72	0.76	1.95	45	3.5	9.55	1316	5.2	1321	Cu-Fe ore
S6	32.4	0.46	0.93	0.11	0.43	1.56	1.5	24.7	2.8	17.35	2455	8.9	2464	Massive Cu-Fe ore
S7	20	0.29	0.79	0.05	0.2	0.49	0.08	14.9	2.1	14.18	167	6.7	173	Carbonate-Quartz rock
S8	170	0.68	1.8	0.04	1.38	0.65	0.71	88.4	3.5	11.06	1364	5.6	1369	Massive Cu-Fe ore
S9	48.3	0.34	0.81	0.08	0.51	0.64	1.59	30.8	1.8	10.18	1236	5.3	1241	Cu-Fe ore
W-15	154	1.03	8.52	4.22	1.34	6.72	-	-	9	17	51	7.3	59	ore, open pit
W-18	12.8	0.55	1.5	0.56	0.22	0.55	-	-	5	10	239	3.6	242	massive ore
W-25	18.1	1.6	6.21	1.22	0.29	3.23	-	-	22	66	189	24.6	213	epid-amph rock
W-31	31.4	3.61	4.58	1.03	1.07	6.04	-	-	16	52	122	20.7	142	skarn
W-31a	6.2	0.26	1.95	0.02	0.02	29.1	-	-	1	11	19	2.4	22	skarn with garnet
Min	4	0.03	0.3	0.01	0.02	0.3	0.08	2.5	1	4.24	19	2	22	
Max	364	5.43	8.52	4.22	4.11	29.1	2.55	294.2	22	81.39	2455	44	2464	
Average	95.6	1.2	2.3	0.3	1.2	2.4	1.1	72.7	4.6	18.6	692	9	701	

Std Dev.	92.4	1.3	1.9	0.7	1.2	5.0	0.7	71.7	4.4	17.9	632	9	634	
W-36	36.1	0.32	1.07	0.24	0.29	1.9	-	-	5	17	542	4.5	546	Cu-concentrate
W-37	36.5	0.42	1.35	0.42	0.37	0.53	-	-	3	15	920	4.5	925	Fe-concentrate
W-39	204	1.94	6.41	1.88	2.17	3	-	-	13	49	2550	18.9	2569	Waste I
W-40	189	1.85	6.23	1.88	2.01	2.7	-	-	13	55	2559	15.8	2575	Waste II
W-44	104	1.39	5.52	1.59	1.15	2.79	-	-	13	99	5450	21	5471	Waste out from tailing

Table 2. Correlation coefficients for ore and impurity elements in the samples from the Sin Quyen deposit (39 samples)

Elements	Cu	Fe	Mn	Co	Ni	Au	Zn	Ag	Pb	Ga	Ge	S	Sn	Te	Tl	Bi	Cd	U	Th	V	REE
Cu	1																				
Fe	**0.53**	1																			
Mn	-0.44	0.1	1																		
Co	0.46	**0.59**	-0.08	1																	
Ni	0.15	0.31	0.05	**0.9**	1																
Au	**0.73**	0.17	-0.12	0.33	0.21	1															
Zn	**0.67**	0.39	-0.09	0.26	-0.04	0.49	1														
Ag	**0.94**	**0.5**	-0.22	0.41	0.11	**0.74**	**0.68**	1													
Pb	**0.82**	0.46	0.22	0.41	0.16	**0.74**	**0.64**	**0.82**	1												
Ga	-0.08	0.28	**0.59**	-0.17	-0.32	-0.05	0.23	0.03	-0.03	1											
Ge	0.11	-0.18	0.33	0.21	0.05	-0.07	0.24	0.21	0.2	0.49	1										
S	0.26	0.2	0.02	**0.83**	**0.77**	0.18	0.2	0.25	0.16	-0.18	0.18	1									
Sn	0.19	0.28	0.18	0.47	**0.55**	0.19	0.29	0.22	0.36	-0.19	0.42	0.39	1								
Te	**0.94**	0.35	-0.22	**0.56**	0.26	**0.69**	**0.7**	**0.93**	**0.82**	0.01	0.29	0.42	0.34	1							
Tl	-0.18	-0.32	0.35	-0.22	-0.22	-0.09	0.13	-0.08	-0.13	**0.61**	0.07	0.14	-0.18	-0.18	1						
Bi	**0.90**	0.14	-0.26	**0.51**	0.23	**0.76**	**0.6**	**0.92**	**0.77**	0.08	0.25	0.4	0.28	**0.91**	**0.53**	1					
Cd	**0.67**	-0.19	-0.05	0.29	0.03	**0.56**	**0.89**	**0.73**	**0.69**	0.13	0.2	0.23	0.33	**0.69**	0.08	**0.66**	1				
U	**0.78**	0.41	-0.23	0.35	0.11	**0.78**	**0.62**	**0.81**	**0.97**	0.03	0.14	0.09	0.31	**0.78**	-0.04	**0.75**	**0.69**	1			
Th	0.08	0.14	-0.35	-0.15	-0.18	-0.03	-0.14	0.18	-0.03	-0.14	-0.24	-0.2	-0.3	0.04	-0.08	0.09	-0.04	-0.03	1		
V	0.39	**0.56**	0.2	0.08	-0.17	0.21	0.34	0.47	0.3	**0.69**	**0.53**	0.1	0.03	0.43	0.46	**0.56**	0.33	0.33	0.03	1	
REE	0.46	0.26	-0.41	0.20	0.08	0.08	0.12	0.48	0.21	-0.27	0.16	0.17	0.14	0.36	-0.17	0.37	0.11	0.21	**0.64**	0.13	1